

## Importance of Coulomb dissociation of the deuteron on nucleon production reactions

D. Ridikas and W. Mittig

*GANIL, BP 5027, F-14076 CAEN Cedex 5, France*

J. A. Tostevin

*Department of Physics, School of Physical Sciences, University of Surrey, Guildford, Surrey, GU2 5XH, United Kingdom*

(Received 21 September 1998)

A narrow beam of high energy neutrons or protons can be produced if a target material is bombarded with energetic deuterons. The processes which lead to the formation of stripped particle beams in encounters of high energy deuterons with target nuclei are briefly reviewed. We show that elastic Coulomb dissociation of the deuteron may play a significant role in energetic and forward peaked neutron/proton production on heavy metal targets. [S0556-2813(99)04003-0]

PACS number(s): 24.10.-i, 21.60.Ka, 25.10.+s, 25.45.-z

### I. INTRODUCTION

Interest in the study of neutron production reactions has been revived recently. They are the basis for the development of powerful neutron sources for multiple purposes, such as nuclear energy generation and incineration of nuclear waste, materials analysis, tritium production, nuclear medicine, etc. [1–4]. A related interest is the possibility of producing radioactive nuclei and exotic beams by neutron induced fissions [5,6].

A narrow beam of energetic neutrons or protons can be produced efficiently by employing an incident deuteron beam. Already in 1947 Serber [7] identified several different processes by which high energy nucleons are ejected when a target is bombarded by high energy deuterons. First, a deuteron passing even at large distances from an atomic nucleus may be disintegrated by its Coulomb field [8]. Second, when a deuteron grazes the edge of the nucleus, the proton may interact and scatter from the nucleus, being stripped from the neutron which then continues with approximately half of the energy of the incident deuteron [7,9]. Finally, high energy ejectiles can be produced by direct collision by one of the nucleons of the deuteron and a nuclear particle [10]. The importance of the first two processes depend primarily on the fact that the deuteron is a very loosely bound system, the proton and neutron actually spending much of their time outside of the range of their mutual interaction.

In this paper we examine energy distributions of neutrons produced in deuteron induced reactions on thin target materials measured experimentally [11] and calculated using the LAHET Code System (LCS) [12]. We show below that a characteristic narrow peak in the cross section for large emitted neutron energies, seen clearly at forward angles and which falls with increasing scattering angle, is not properly reproduced by the LCS for deuterons on heavy targets. Similar conclusions were drawn also in [11], where simulations were performed with the code of Cugnon [13]. There the authors clearly state that their model neglects the coherent dissociation of the incident deuteron. This process, basically due to the Coulomb forces, is expected to enhance the high energy neutron yield at very forward angles. We note that the recent discovery [14] of very extended halo nuclei with a dense

charged core and one, or sometimes two, very loosely bound valence neutrons, has renewed interest in methods for the calculations of this Coulomb dissociation mechanism. This is believed to be a significant reaction channel in the scattering of such nuclei from heavy targets.

The paper is organized as follows. In Sec. II we briefly recall the main ingredients of the IntraNuclear Cascade (INC) model employed by the LCS. Section III outlines an elastic Coulomb dissociation model applicable for weakly bound two-body systems at the energies of interest here. Section IV presents our results for the neutron or proton angular and energy distributions which are compared to experimental data where available. The results are summarized in Sec. V.

### II. LIGHT PARTICLE PRODUCTION WITHIN THE LCS

In 1947 Serber [10] proposed a two stage picture of spallation reactions. In the first (fast) stage the incident particle loses part of its energy by individual nucleon-nucleon collisions. In the second (slow) stage target excitation energy is released by evaporation. The component in the particle spectra extending between the evaporation bump and the quasi-elastic peak is then due to multiple collisions in this description.

Here, within the LCS [12], we consider in more detail only the first stage, often referred as an intranuclear cascade (INC) (see, for example, Refs. [15–17] for more details). An alternative to the Bertini INC model [15], LAHET contains the INC routines from the ISABEL code [18] and has the capability of treating nucleus-nucleus as well as particle-nucleus interactions. In the present implementation of the LCS, only projectiles with  $A \leq 4$  are allowed.

In short, the INC model pictures the nuclear collision process as a sequence of binary baryon-baryon collisions, occurring as in free space. The target is seen as a continuous medium which presents a mean free path  $\lambda = (\rho\sigma)^{-1}$  to the particles. After travelling one path length, the particle is expected to scatter on a nucleon, which is promoted to the continuum. Both target and projectile Fermi motions, Pauli blocking of collisions leading to already occupied states, inelastic collisions and pion production, and the effects of the target mean field are included. Thus the active particles are

propagated, in small steps, and their collisions are described stochastically. Energy, momentum, baryon number, and charge conservation are also present in the LCS (see Ref. [12] for more details).

The picture is nearly the same for deuterons except that the projectile must now be constructed by choosing at random the relative coordinate and momentum of the neutron and proton. These are taken as Gaussian distributions, the widths of which are consistent with the known properties of the deuteron. The center of mass of the projectile is then boosted with the appropriate velocity and impact parameter [18].

For projectiles with  $A=2$  (or 3) the LCS uses the true average binding energy per nucleon. For heavier nuclei it uses the average binding energy of the last neutron and the last proton (actually the average of the  $p$  and  $n$  separation energies) [19]. So, in principle, the loosely bound nature of the deuteron,  $E_s=2.23$  MeV, is correctly taken into account. The major problem with light nuclei, however, might be that no provision is made for isotope-specific projectile nuclear density distributions. For both the projectile and target they are described as a function of  $A$  appropriate only for heavier masses [18]. The cascade particles, in the region of overlap between the projectile and target, are followed until they leave the region— independent of their kinetic energy. Outside the overlap region however they are followed until they either leave the projectile and target volume, or their energy falls below a cutoff energy for the particle escape [18]. The neutron cutoff energy is uniformly distributed between zero and twice the mean binding energy. The Coulomb barrier is randomly distributed in a form simulating a Coulomb barrier transmission probability, the maximum of the Coulomb barrier and the neutron cutoff is then used as the proton cutoff energy [12].

Since the INC model deals only with two-body reactions, depending on spatial overlap, either one or both of the projectile nucleons can interact with a nucleon in the target. Thus there is a probability of both “stripping” or “pickup” with a deuteron. However there is no special mechanism included to the ground state and both projectile and target usually suffer further disintegration [19]. This is not the case for the elastic breakup  $A(d,np)A_{g.s.}$  reaction in which deuteron dissociation takes place via the Coulomb field, leaving the target nucleus in its ground state. We present briefly our treatment of the Coulomb dissociation process in the following section.

### III. ELASTIC COULOMB DISSOCIATION OF THE DEUTERON

For the calculation of the differential cross sections for deuteron Coulomb disintegration we make use of the adiabatic model proposed in [20] and discussed fully in [21]. The theoretical model used makes only the single approximation that the neutron-proton relative energies excited by the target Coulomb interaction are small in comparison with the incident energy of the deuteron—also referred to as the sudden approximation.

The advantage of this model, in the present context, is that it leads to a closed form expression for the quantum mechanical Coulomb breakup transition amplitude which can be

computed very efficiently. These model calculations have been shown [20,21] to lead to a very good quantitative agreement with experimental data [22] for elastic breakup of the deuteron, at 140 MeV and 270 MeV, measured in a very forward angles geometry where the Coulomb breakup mechanism is expected to be dominant. The agreement with experiment extended over the full spectrum of possible emerging proton energies and for targets from  $^{12}\text{C}$  to  $^{208}\text{Pb}$ . The finite sizes of the detectors in those experiments extended the measurements to proton angles of order  $4^\circ$  in the laboratory frame.

Since this model calculates the elementary triple differential cross section, with respect to the two nucleon solid angles and one nucleon energy, in the following these calculated triple differential cross sections must be integrated over neutron and/or proton angles and/or energy to compare with more inclusive observables. Clearly at large angles for the emerging nucleons the cross sections will also be affected by nuclear distortions. The nuclear parts of the interactions are taken into account by the standard LCS modelling. In all cases we calculate the additional cross sections for pure Coulomb dissociation in the absence of nuclear interactions, assuming non-relativistic kinematics.

### IV. DEUTERON INDUCED NUCLEON PRODUCTION AT FORWARD ANGLES

Neutrons and protons from the  $A(d,np)A_{g.s.}$  elastic Coulomb breakup process are ejected in a strongly confined angular and energy region, i.e., at very forward angles and with approximately half the incident deuteron energy. Therefore, to study the importance of this process within the LCS, we compare the calculated and measured energy spectra for neutron production at zero degrees. The experiment [11] was performed at the synchrotron of the Laboratoire National Saturne (LNS). The time structure of the beam delivered by the synchrotron did not allow conventional time-of-flight (TOF) measurements, so, neutron energy spectra were measured using two different techniques, described in more detail in [23,24]. Low energy neutrons ( $E_n \leq 400$  MeV; represented by diamonds hereafter) were measured using the TOF between the tagged beam particles and the neutrons detected in a thick liquid scintillator. The high energy neutrons ( $E_n \geq 200$  MeV; represented by squares hereafter) were measured with a liquid hydrogen converter, i.e., via  $(n,p)$  scattering, and a magnetic spectrometer. It has to be noted that the two experimental techniques are independent and, in the 200–400 MeV range where they overlap, they agree within 20%. As we will show later, our simulations also confirm, independently, the absolute values of these energy distributions in this energy region.

Figures 1 and 2 show neutron energy spectra, at zero degrees in the laboratory frame, from 1200 MeV deuterons interacting with Pb and Fe targets, respectively. In the case of the Pb target (see Fig. 1 and its lower part in particular), in the peak of the energy distribution at around 600 MeV neutron energy, the calculated Coulomb  $(d,np)$  (dotted curve) and LAHET (stars) cross sections are very similar in magnitude. The experimentally measured peak is nearly a factor of two greater (squares). Upon summing the LAHET and Coulomb dissociation terms one obtains (solid curve) an excel-

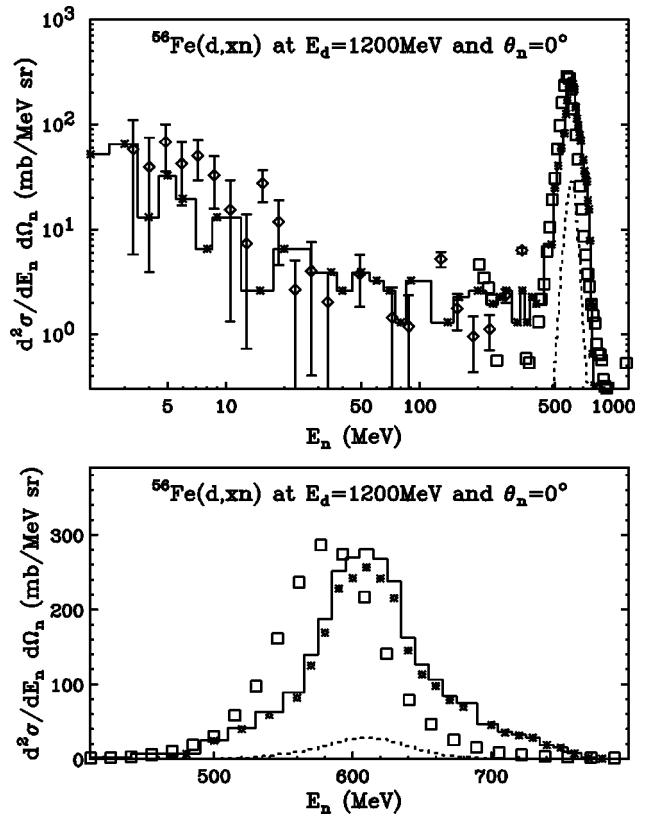
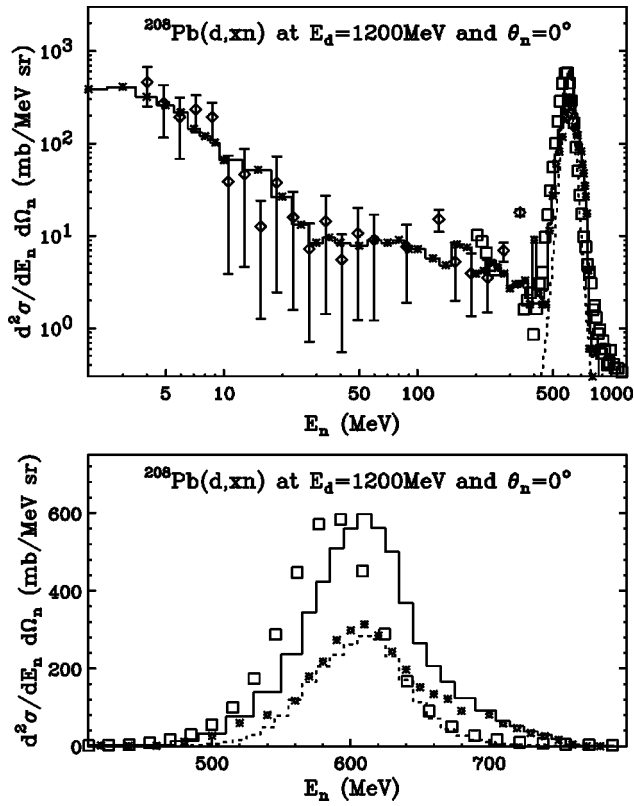


FIG. 1. Neutron energy distribution at zero degrees in the laboratory frame from 1200 MeV deuterons interacting with a lead target (upper part) together with its characteristic narrow peak for large emitted neutron energies (lower part) in a linear scale. Stars and dotted lines represent the distributions of the total  $n$  production calculated with the LCS and the  $n$  production from the Coulomb breakup of the deuteron, leaving the target nucleus in its ground state, respectively. The solid line is the sum of the LCS and Coulomb contributions. The experimental data (squares and diamonds) are from [11].

FIG. 2. As for Fig. 1 but for 1200 MeV deuterons interacting with iron target.

lent agreement with the experimental data (squares and diamonds). In the case of the Fe target (see Fig. 2 and its lower part in particular) the elastic Coulomb disintegration cross section is of course considerably smaller, due to the smaller target charge, and the LAHET contribution alone (stars) gives a reasonable description of the data (squares and diamonds). Note that the experimental points are slightly shifted to the lower energy (see lower parts of Figs. 1 and 2 in particular) since they are not corrected for deuteron and nucleon energy losses inside the target material [11].

To clarify up to which angles the deuteron Coulomb dissociation is important for calculations of the total neutron production, in Fig. 3 we plot neutron angular spectra for the same deuteron energy and targets as above. For the Pb target (two upper curves) Coulomb dissociation (dotted line) yields a contribution comparable to that from LAHET (solid line) for angles from  $0^\circ$  to  $8^\circ$  in the laboratory frame. As expected, for the Fe target (two lower curves), already at  $0^\circ$  the LAHET calculation (dashed line) gives good agreement with experiment and the Coulomb breakup contribution (dot-dashed line) is of minor importance. For both the Fe and Pb targets we should note that the total neutron production cross section  $\sigma$  (LAHET), as estimated using the LCS, is larger by 2

orders of magnitude than the angle and energy integrated deuteron elastic Coulomb dissociation cross section  $\sigma$  ( $n$  elastic). The numbers are given in Fig. 3. This emphasizes the very localized nature, in energy and angular range, of the Coulomb contribution.

In the absence of data the discussion above becomes more qualitative when one lowers the energy of the incident deu-

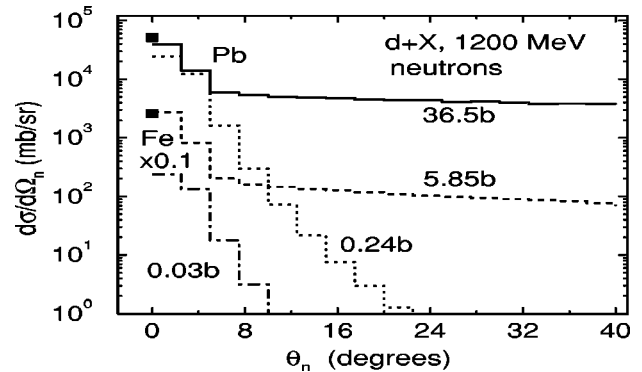


FIG. 3. Energy integrated neutron production cross sections for 1200 MeV deuterons interacting with a lead target (two upper curves) and an iron target (two lower curves, scaled by 0.1). The solid and dashed curves represent the distributions of the total  $n$  production calculated with the LCS. The dotted and dot-dashed curves show the distributions of  $n$  production from the Coulomb breakup of the deuteron, leaving the target nucleus in its ground state. Experimental data (squares) are from [11]. The total neutron production cross sections are shown in each case.

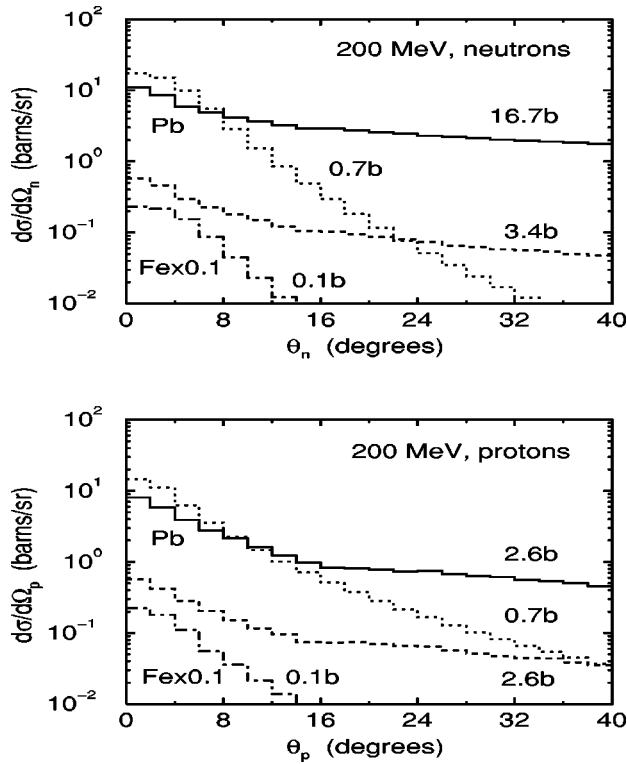


FIG. 4. Energy integrated neutron (upper part) and proton (lower part) production cross sections in the laboratory frame from 200 MeV deuterons interacting with a lead target (two upper curves) and an iron target (two lower curves, scaled by 0.1). The solid and dashed curves represent the distributions of the total  $n$  and  $p$  production calculated with the LCS. The dotted and dot-dashed curves show the distributions of  $n$  and  $p$  production from the Coulomb breakup of the deuteron, leaving the target nucleus in its ground state. The total  $n$  and  $p$  production cross sections are shown in each case.

terons, and also compares cross sections for proton production in a similar manner. Firstly, our calculations show that both the neutron ( $d, xn$ ) and proton ( $d, xp$ ) production cross sections decrease with deuteron energy while the integrated  $A(d, np)A_{g.s.}$  Coulomb breakup cross section increases. This would indicate that the latter process is relatively more important in the total nucleon production. Secondly, at lower incident energies both the neutrons and protons from deuteron disintegration have a greater probability of suffering multiple collisions before leaving the target nucleus, which is now less transparent. The angular distributions of the emitted nucleons thus become broader (for protons in particular due to the Coulomb interaction). This feature is very important from the experimental point of view since the measurements of proton energy spectra become much more complicated at very forward angles.

In Figs. 4 and 5 we present results analogous to those in Fig. 3. Now however we plot the neutron (upper parts) and proton (lower parts) angular distributions, for Fe and Pb targets, at incident deuteron energies of 200 MeV (Fig. 4) and 100 MeV (Fig. 5), respectively. In this energy range, the Coulomb dissociation of the deuteron becomes important at very forward angles for the Fe target also (compare dashed and dot-dashed lines). On the other hand, this process contributes less than 5% for neutrons and less than 7% for pro-

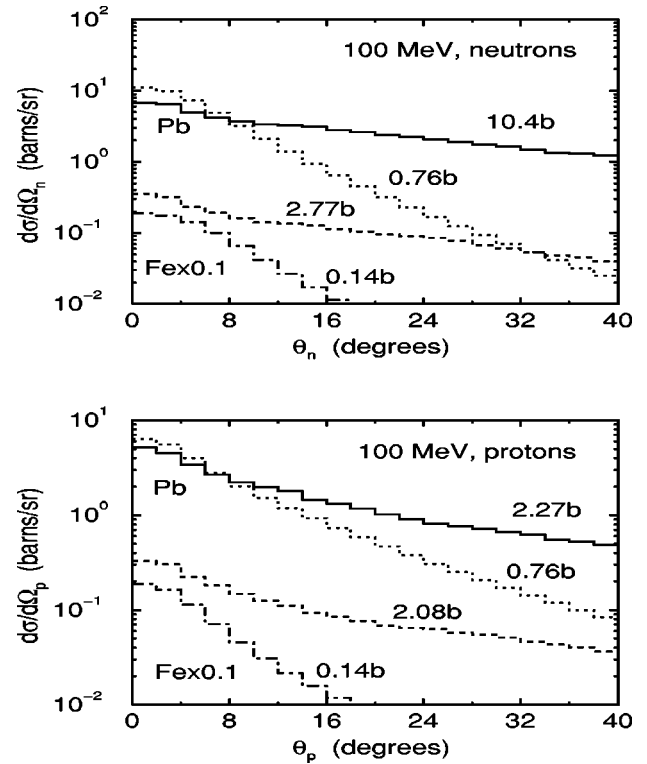


FIG. 5. As for Fig. 4 but for 100 MeV deuterons interacting with lead and iron targets.

tons, when compared to the total nucleon production cross sections estimated by the LCS.

In the case of a heavy (Pb) target however the Coulomb dissociation may dominate at very forward angles, as is shown in Figs. 4 and 5. Moreover, it contributes between 7% (in the case of neutrons) and 34% (in the case of protons) to the corresponding total nucleon production cross sections calculated using the LCS. The discussion above, and in particular the last example, shows clearly that significant cross sections from elastic Coulomb breakup of the deuteron on heavy metal targets ( $Z > 26$ ) are missing from the LCS model. Good quality forward angle nucleon production data are required to confirm these estimates.

## V. SUMMARY

We have presented a brief survey of nucleon production calculations for deuteron induced reactions in the 100–1200 MeV range. We have shown that a characteristic narrow peak in the energy distribution for large emitted nucleon energies, seen clearly in zero degree data, is not properly reproduced by calculations using the LAHET Code System (LCS) in the case of heavy metal targets. We believe that the LCS modelling neglects the coherent Coulomb dissociation of the incident deuteron and that this process enhances the high energy nucleon yield at very forward angles. By adding incoherently the Coulomb dissociation cross section to that calculated using the LCS we obtain an excellent agreement with the magnitudes of the available data.

We estimate that the Coulomb dissociation contributes up to 7% of the cross section in the case of neutron production and up to 34% in the case of proton production, depending

on the target material and the energy of incident deuteron. To confirm these predictions and to clarify up to which angles the process is important for calculations of the total nucleon production, good quality forward angle data are required. In addition, simple parametrization formulas could be derived to allow the Coulomb dissociation to be incorporated within the LCS calculation.

#### ACKNOWLEDGMENTS

We wish to express our appreciation to Dr. R. E. Prael (Los Alamos National Laboratory) for providing us with the LAHET Code System, and his help in the interpretation of the results. The authors are also grateful to Dr. E. Martinez (Laboratoire National Saturne) for providing the experimental data used here in tabular form.

- 
- [1] C. D. Bowman *et al.*, Nucl. Instrum. Methods Phys. Res. A **320**, 336 (1992).
- [2] G. S. Bauer, Proceedings of the 2nd International Conference on Accelerator-Driven Transmutation Technologies and Applications, Kalmar, Sweden, 1996.
- [3] H. Nifenecker and M. Spiro, "Hybrid systems for waste incineration and/or energy production," Journées GEDEON, Cadarache, 1997.
- [4] D. Ridikas and W. Mittig, Nucl. Instrum. Methods Phys. Res. A **418**, 449 (1998); GANIL Report No. GANIL P 98 02, 1-22 (1998).
- [5] J. A. Nolen, in *Proceedings of the 3rd International Conference on RNB*, Gif-sur-Yvette, France, 1993, edited by D. J. Morrissey (Editions Frontières, Gif-sur-Yvette, France, 1993), p. 111; and Concept for Advanced Exotic Beam Facility Based on ATLAS, Argonne National Laboratory, 1995.
- [6] D. Ridikas and W. Mittig, in *Second International Conference on Exotic Nuclei and Atomic Masses (ENAM'98)*, edited by Brad M. Sherril, David J. Morrissey, and Cary N. Davids, AIP Conf. Proc. No. 455 (AIP, New York, 1998); D. Ridikas and W. Mittig, GANIL Report No. GANIL P 98 22, 1-25 (1998).
- [7] R. Serber, Phys. Rev. **72**, 1008 (1947).
- [8] S. M. Dancoff, Phys. Rev. **72**, 1117 (1947).
- [9] R. J. Glauber, Phys. Rev. **99**, 1515 (1955).
- [10] R. Serber, Phys. Rev. **72**, 1114 (1947).
- [11] E. Martinez, These le Grade de Docteur de l'Universite de Caen, Caen, 1997; available by request from DPTA/SPN, Commissariat à l'Energie Atomique (CEA), 91680 Bruyères-le-Châtel, France.
- [12] R. E. Prael and H. Lichtenstein, "User Guide to the LCS: the LAHET Code System," Los Alamos National Laboratory Report LA-UR-89-3014, 1989.
- [13] J. Cugnon, C. Volant, and S. Vuillier, Nucl. Phys. **A625**, 729 (1997).
- [14] I. Tanihata *et al.*, Phys. Lett. **160B**, 360 (1985); I. Tanihata *et al.*, Phys. Rev. Lett. **55**, 2676 (1985); I. Tanihata *et al.*, Phys. Lett. B **206**, 592 (1988).
- [15] H. W. Bertini, Phys. Rev. **188**, 1711 (1969).
- [16] F. M. Waterman *et al.*, Phys. Rev. C **8**, 2419 (1973).
- [17] J. Cugnon, Nucl. Phys. **A462**, 751 (1987).
- [18] Y. Yariv and Z. Fraenkel, Phys. Rev. C **20**, 2227 (1979).
- [19] R. E. Prael (private communication).
- [20] J. A. Tostevin *et al.*, Phys. Lett. B **424**, 219 (1998).
- [21] J. A. Tostevin, S. Rugmai, and R. C. Johnson, Phys. Rev. C **57**, 3225 (1998).
- [22] H. Okamura *et al.*, Phys. Lett. B **325**, 308 (1994); H. Okamura *et al.*, Phys. Rev. C **58**, 2180 (1998).
- [23] F. Borne *et al.*, Nucl. Instrum. Methods Phys. Res. A **385**, 339 (1997).
- [24] E. Martinez *et al.*, Nucl. Instrum. Methods Phys. Res. A **385**, 345 (1997).